

Transport model based on inputs from chiral effective theory

Che-Ming Ko
Texas A&M University

- Introduction: chronology of heavy ion collisions
- High energy heavy ion collisions: nuclear equation of state
- Collisions with neutron-rich nuclei: nuclear symmetry energy
- Test of chiral nuclear interactions in heavy ion collisions
- Summary



Chronology of heavy ion collisions

- 1970's: below Coulomb barrier → deeply inelastic collisions; nuclear dissipation and damping of collective motions
- 1980's: high energies ($\sim 1-2$ GeV/nucleon @ fixed target, Bevalac); nuclear equation of state at high densities ($\sim 3\rho_0$)
- 1990's: high (GSI) and relativistic ($\sim 10-100$ GeV/nucleon @ fixed target, AGS, SPS); nuclear equation of state ($\sim 5\rho_0$) and quark-gluon plasma
- 2000's: ultrarelativistic energies ($\sim 100-200$ GeV/nucleon @ c.m., RHIC) → nearly baryon-free quark-gluon plasma; neutron-rich nuclei (MSU, GSI) → nuclear symmetry energy ($\sim \rho_0$)
- 2010's: ultrarelativistic energies (~ 5 TeV/nucleon @ c.m., LHC) → baryon-free quark-gluon plasma
- 2020's: relativistic energies (~ 10 GeV/nucleon @ c.m., FAIR) → baryon-rich quark-gluon plasma; medium energies (~ 250 MeV/nucleon @ fixed target, FRIB) → nuclear symmetry energy ($\sim 2.5\rho_0$)

Nuclear equation of state

Li, Chen & Ko, Phys. Rep. 464, 113 (2008)

EOS of asymmetric nuclear matter

$$E(\rho, \delta) \approx E_0(\rho) + E_{\text{sym}}(\rho)\delta^2, \quad \delta = \frac{\rho_n - \rho_p}{\rho_n + \rho_p}$$

EOS of symmetric nuclear matter

$$E_0(\rho) \approx E_0(\rho_0) + \frac{1}{2}K_0 \left(\frac{\rho - \rho_0}{3} \right)^2, \quad \rho_0 \approx 0.16 \text{ fm}^{-3}$$

Symmetry energy

$$E_{\text{sym}}(\rho) = E_{\text{sym}}(\rho_0) + L \left(\frac{\rho - \rho_0}{3\rho_0} \right) + \frac{K_{\text{sym}}}{2} \left(\frac{\rho - \rho_0}{3\rho_0} \right)^2 + \frac{J_{\text{sym}}}{6} \left(\frac{\rho - \rho_0}{3\rho_0} \right)^3 \dots$$

Symmetry energy coefficient

$$E_{\text{sym}}(\rho_0) \approx 30 \text{ MeV} \quad \text{from mass formula}$$

Slope

$$L = 3\rho_0 \left. \frac{\partial E_{\text{sym}}(\rho)}{\partial \rho} \right|_{\rho=\rho_0}$$

theoretical values -50 to 200 MeV

Curvature

$$K_{\text{sym}} = 9\rho_0^2 \left. \frac{\partial^2 E_{\text{sym}}(\rho)}{\partial^2 \rho} \right|_{\rho=\rho_0}$$

theoretical values -700 to 466 MeV

Nuclear matter Incompressibility

$$K(\delta) = K_0 + K_{\text{asy}}\delta^2, \quad K_{\text{asy}} = K_{\text{sym}} - 6L$$

Empirically,

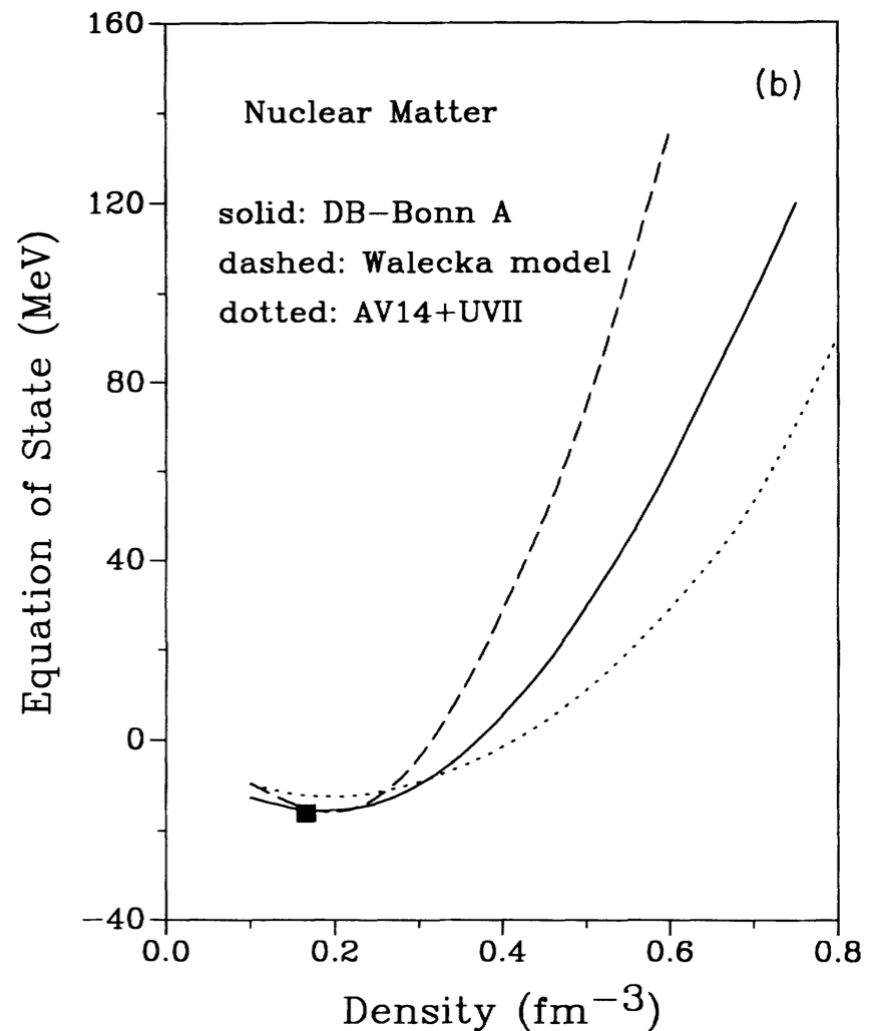
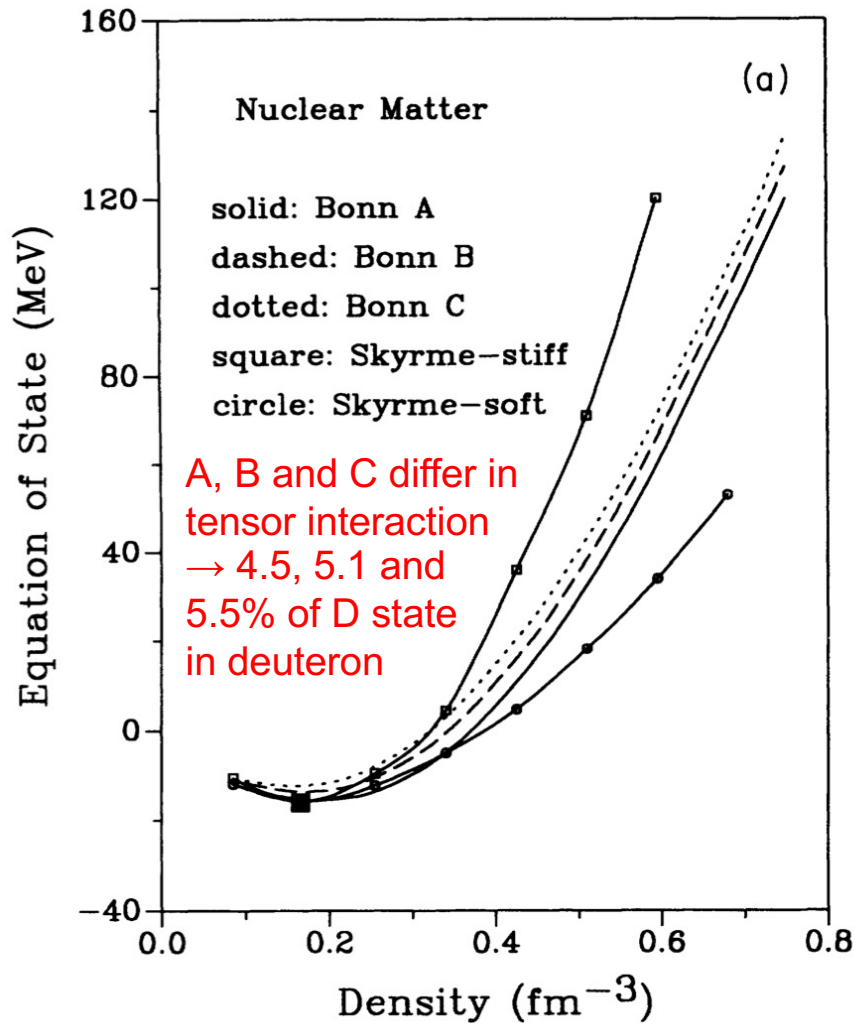
$$K_0 \sim 230 \pm 10 \text{ MeV}, \quad K_{\text{asy}} \sim -500 \pm 50 \text{ MeV}, \quad L \sim 88 \pm 50 \text{ MeV}$$

$$E_{\text{sym}}(\rho) \sim 32 (\rho/\rho_0)^\gamma \quad \text{with } 0.7 < \gamma < 1.1 \text{ for } \rho < 1.2\rho_0$$

- Symmetry energy at high densities is practically undetermined !

Equation of state of symmetric nuclear matter

Li, Machleidt & Brockmann, PRC 45, 2782 (1992)



- Large uncertainties at high densities or in the stiffness of nuclear matter equation of state

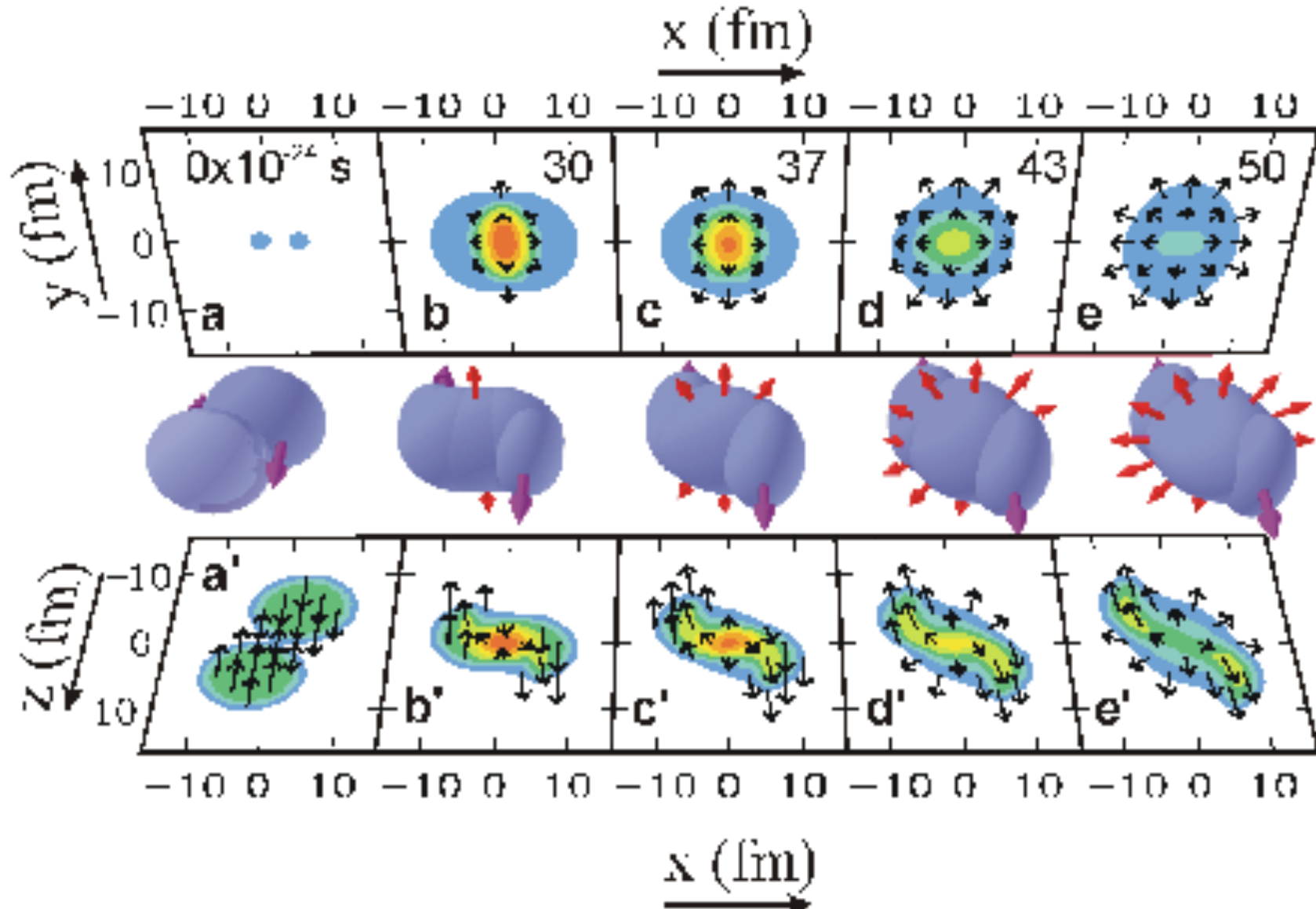
Boltzmann-Uehling-Uhlenbeck model

Bertsch & Das Gupta, Phys. Rep. 160, 189 (1988)

$$\begin{aligned} \frac{\partial f(\mathbf{r}, \mathbf{p}, t)}{\partial t} + \mathbf{v} \cdot \nabla_{\mathbf{r}} f - \nabla_{\mathbf{r}} U \cdot \nabla_{\mathbf{p}} f &= \left(\frac{\partial f}{\partial t} \right)_{\text{coll}} \\ &= \frac{4}{(2\pi)^3} \iint d\mathbf{p}_2 d\mathbf{p}_3 \int d\Omega |\mathbf{v}_{12}| \frac{d\sigma}{d\Omega} (\mathbf{p}_2 - \mathbf{p}_4) \delta(\mathbf{p} + \mathbf{p}_2 - \mathbf{p}_3 - \mathbf{p}_4) \\ &\quad \times \{ f(\mathbf{r}, \mathbf{p}_3, t) f(\mathbf{r}, \mathbf{p}_4, t) [1 - f(\mathbf{r}, \mathbf{p}, t)] [1 - f(\mathbf{r}, \mathbf{p}_2, t)] \\ &\quad - f(\mathbf{r}, \mathbf{p}, t) f(\mathbf{r}, \mathbf{p}_2, t) [1 - f(\mathbf{r}, \mathbf{p}_3, t)] [1 - f(\mathbf{r}, \mathbf{p}_4, t)] \} \end{aligned}$$

- $F(\mathbf{r}, \mathbf{p}, t)$: nucleon distribution function
- $U(\mathbf{r})$: nuclear mean-field potential
e.g., Skyrme potential $U = \alpha \rho(\mathbf{r}) + \beta \rho^{4/3}(\mathbf{r})$
- $d\sigma/d\Omega$: nucleon-nucleon scattering cross sections

Collective flow in heavy ion collisions



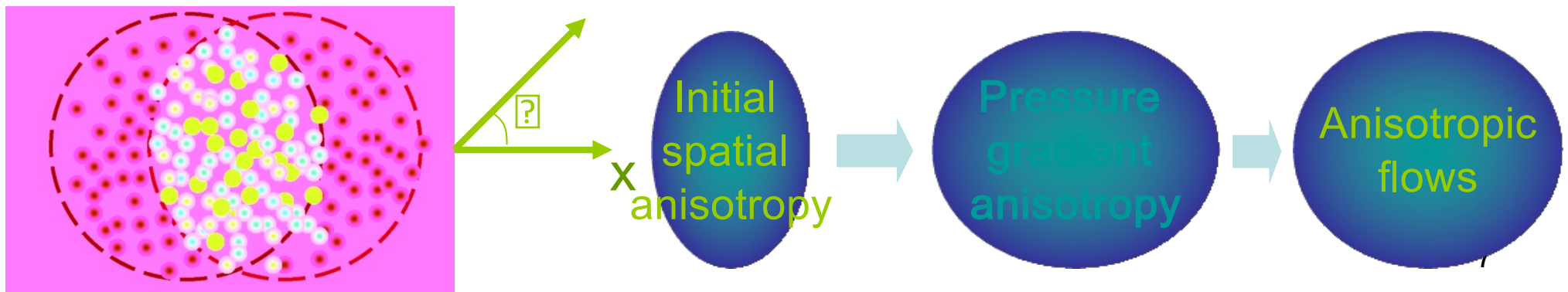
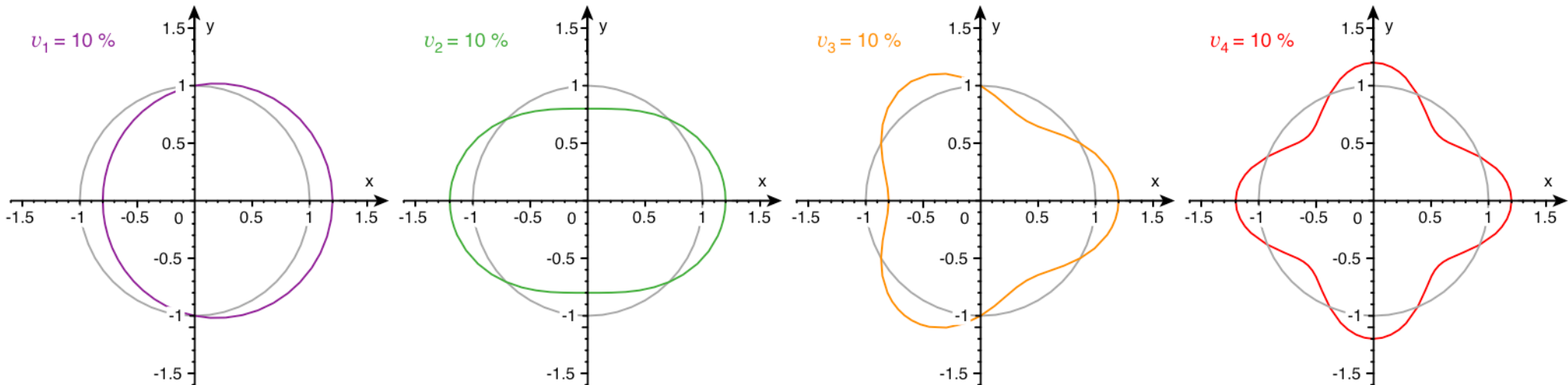
- Directed flow in the reaction (x-z) plane and elliptic flow in the transverse (x-y) plane.

Anisotropic flow

Anisotropic flow v_n

$$E \frac{d^3N}{d^3\vec{p}} = \frac{dN}{p_T dp_T d\varphi dy} = \frac{1}{2\pi} \frac{dN}{p_T dp_T dy} \left[1 + \sum_{n=1}^{\infty} 2v_n(p_T, y) \cos(n\varphi) \right]$$

Sine terms vanish because of the symmetry $\Phi \rightarrow -\Phi$ in A+A collisions

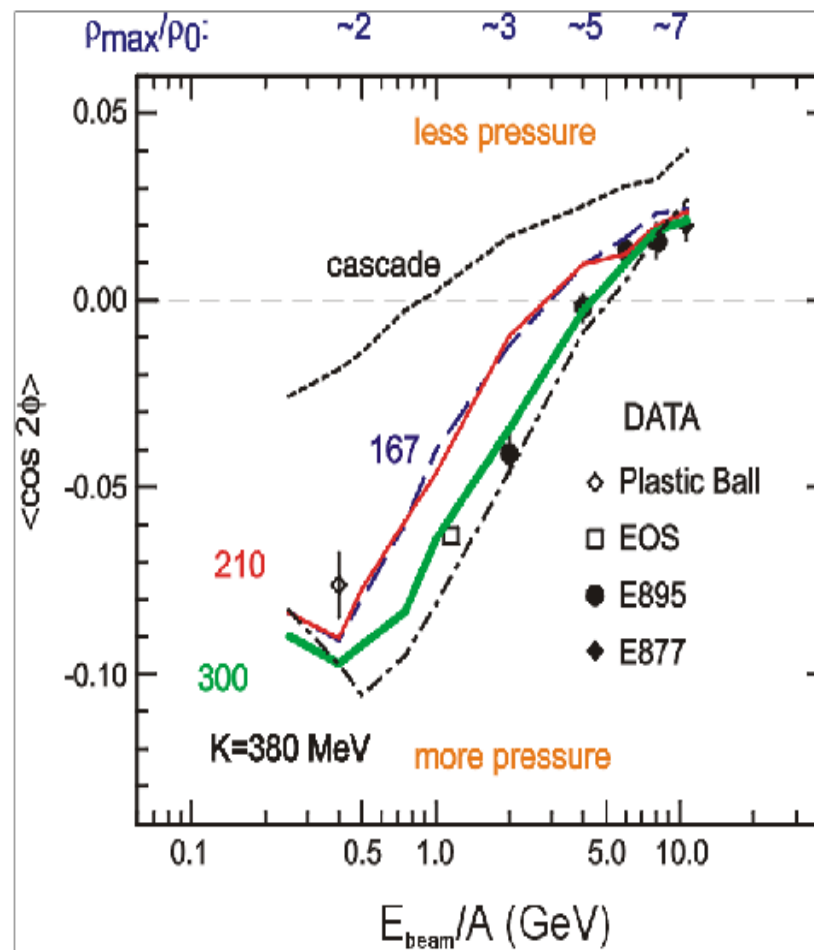
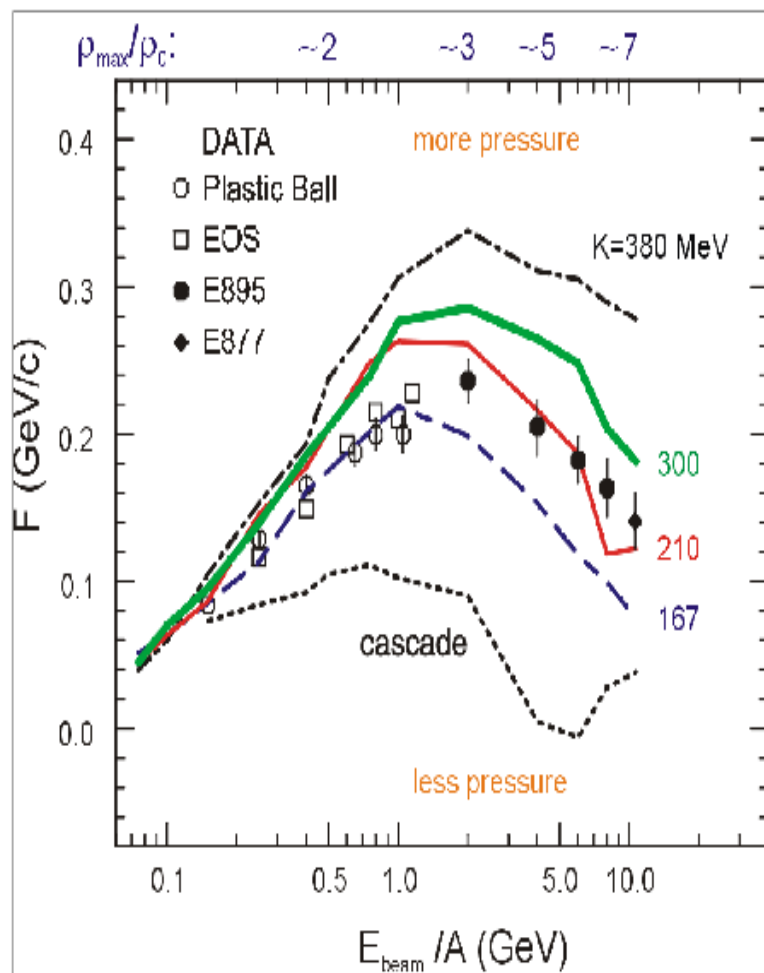


Direct and elliptic flows

Danielewicz, Lacey & Lynch, Science 298, 1592 (2002)

$$\text{Direct flow } F = \left(\frac{dp_x}{dy} \right)_{y_{cm}}$$

$$\text{Elliptic flow } v_2 = \langle \cos 2\phi \rangle = \left\langle \frac{p_x^2 - p_y^2}{p_x^2 + p_y^2} \right\rangle$$

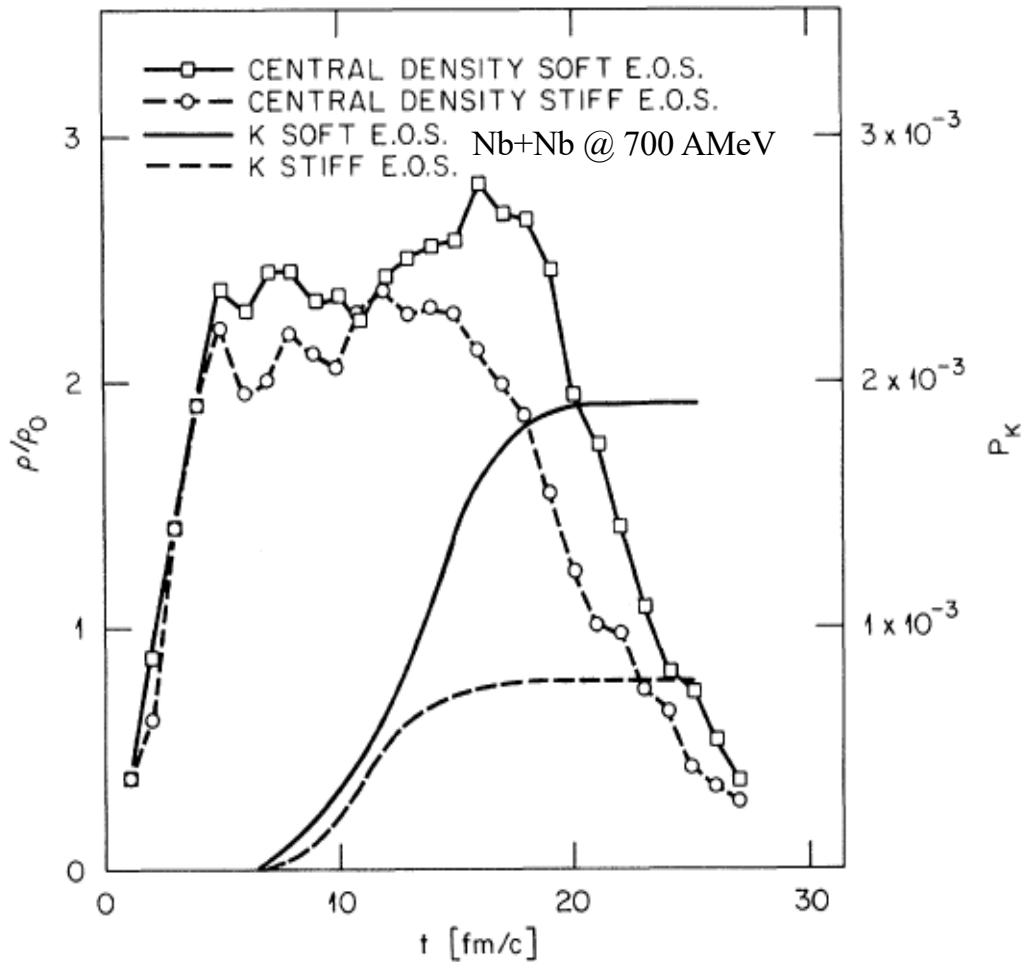


$$E_0(\rho) = E_0(\rho_0) + \frac{K_0}{2} \left(\frac{\rho - \rho_0}{3\rho_0} \right)^2 + \frac{J_0}{6} \left(\frac{\rho - \rho_0}{3\rho_0} \right)^3$$

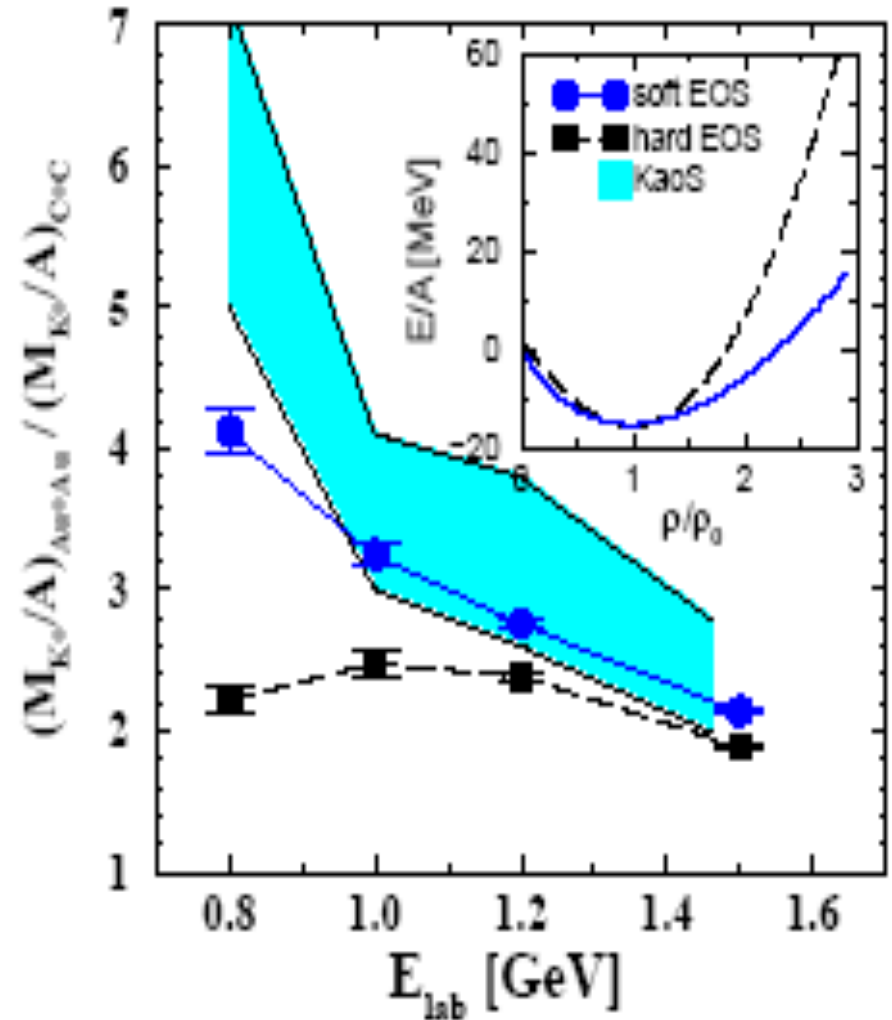
- Data consistent with a nuclear EOS with $K_0 \approx 200 - 300 \text{ MeV}$.

Subthreshold kaon production

Aichelin & Ko, PRL 55, 2661 (1985)



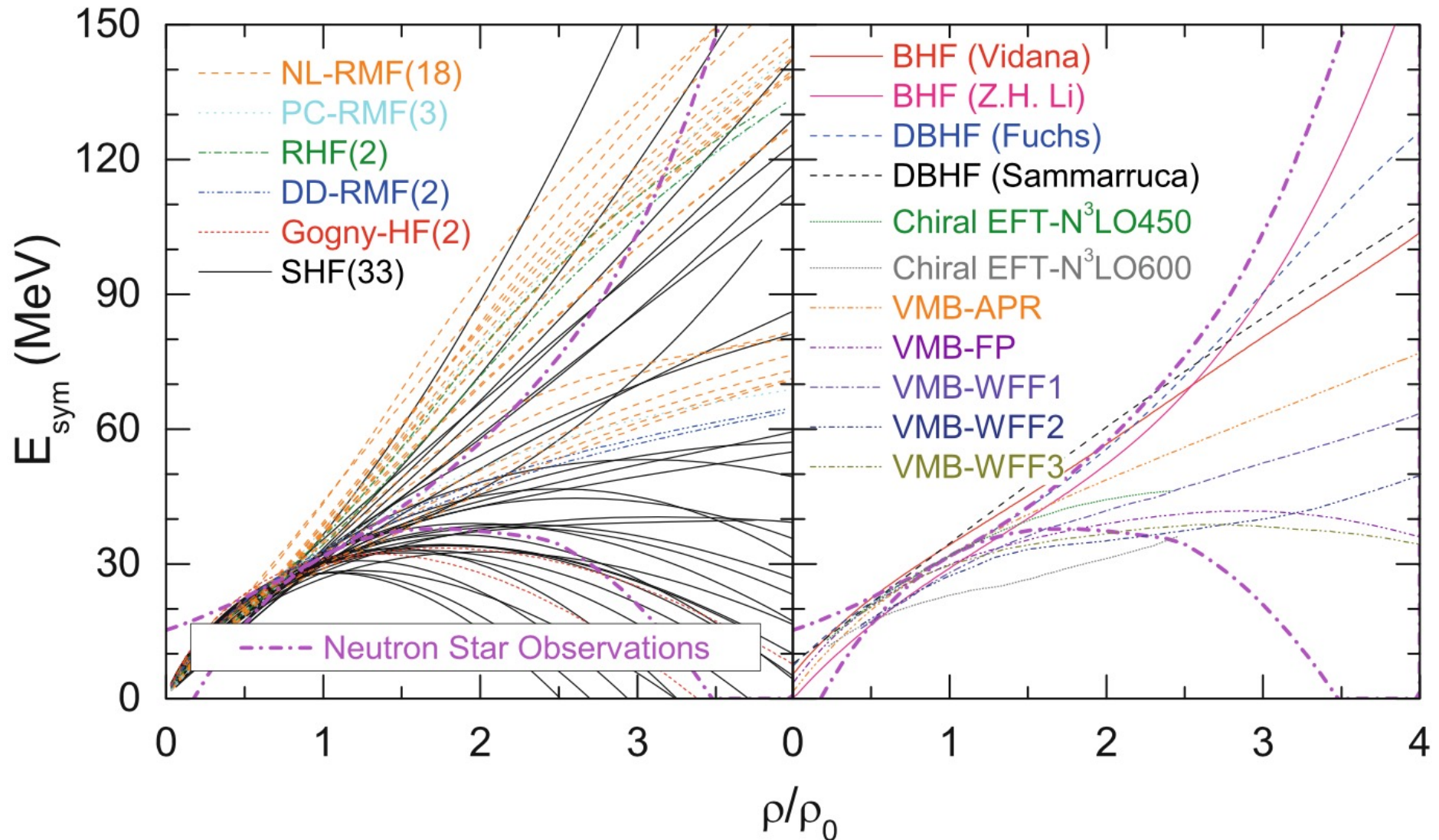
Fuchs, PRL 86, 1974 (2001)



- Kaon production at subthreshold energy in HI collisions is sensitive to nuclear EOS and data are consistent with a soft one,

Theoretical predictions on nuclear symmetry energy

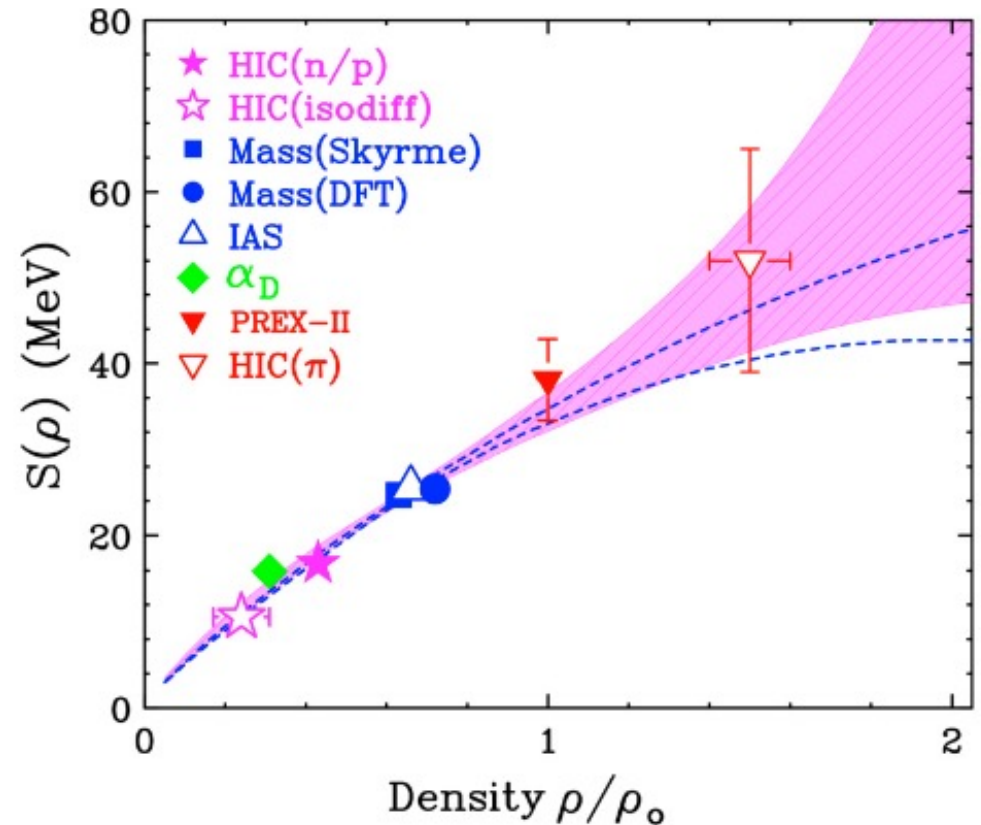
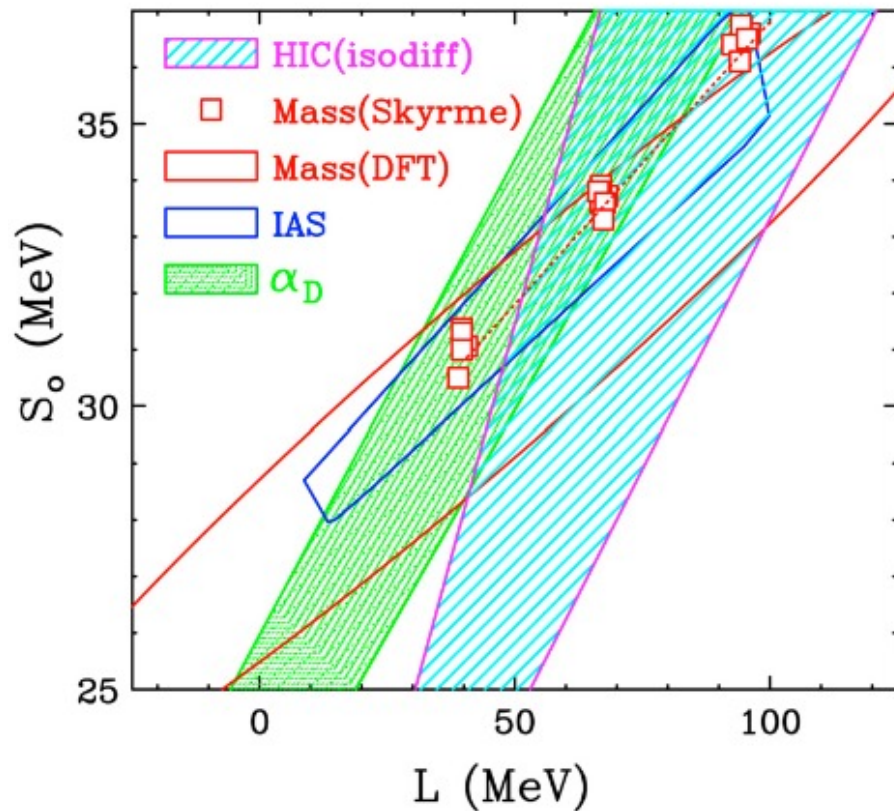
Zhang & Li, EJPA 55, 39 (2019)



■ Large uncertainties at both low and high densities

Density dependence of nuclear symmetry energy

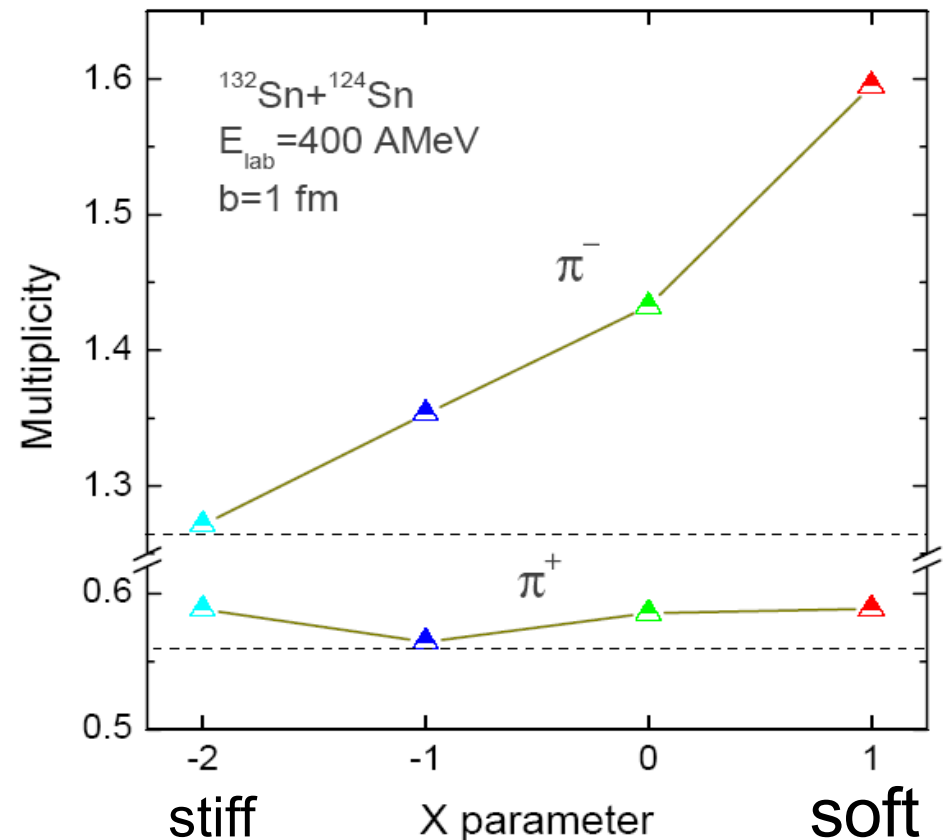
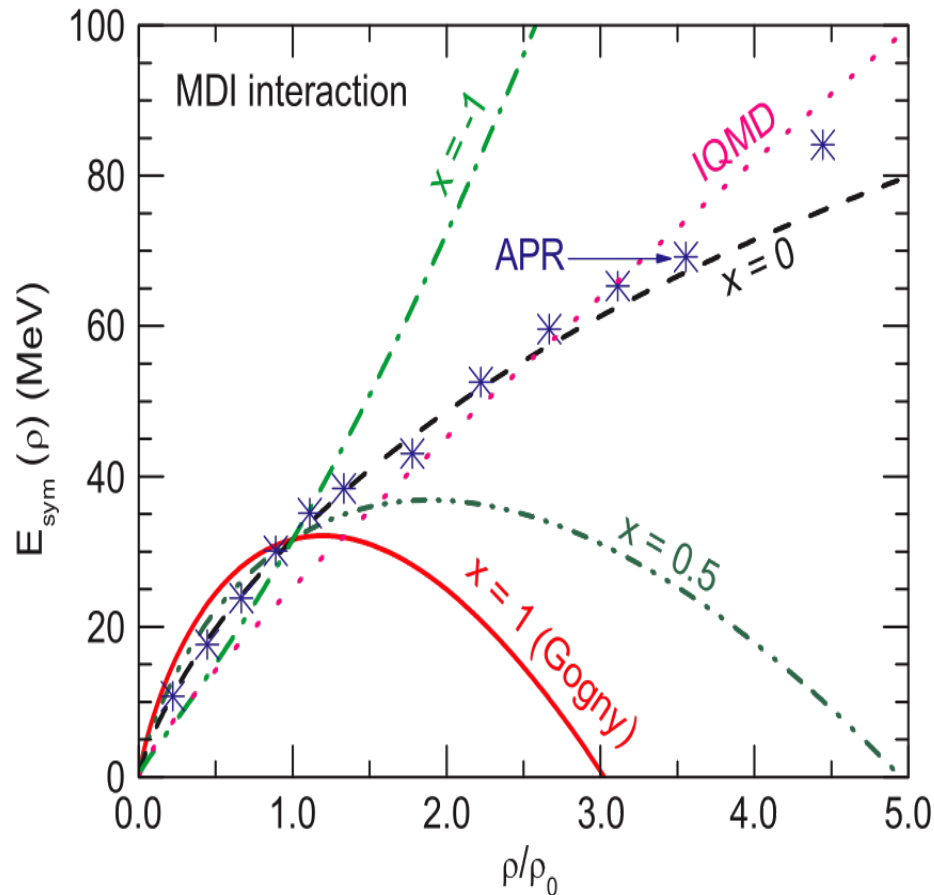
W. G. Lynch and M. B Tsang, PLB 830, 137098 (2022)



- Instead of constraining the symmetry energy S_0 and its slope parameter L at nuclear matter saturation density (left figure), each measured observable should be used to determine the symmetry energy at the density it is most sensitive (right figure).

Near-threshold pion production with high energy radioactive beams (IBUU)

B. A. Li, PRL 88, 192701 (2002)

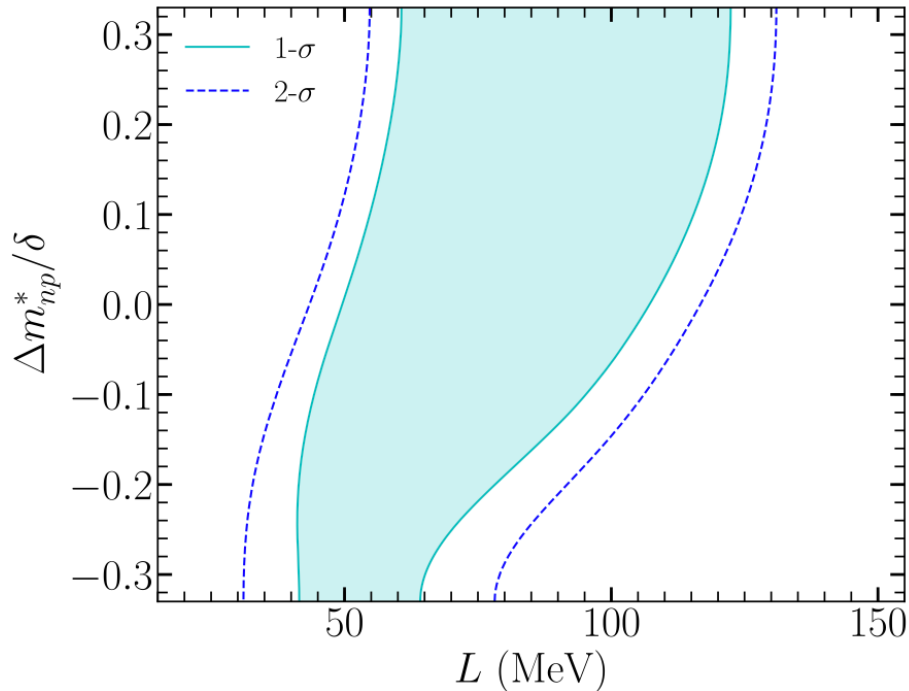


π^- yield is sensitive to the symmetry energy $E_{\text{sym}}(\rho)$ since they are mostly produced in the neutron-rich region, with softer one giving more π^- than stiffer one. Difference between π^-/π^+ from super soft ($x = 1$) and super stiff ($x = -1$) $E_{\text{sym}}(\rho)$ is, however, only about 30%, which makes it very challenging to determine $E_{\text{sym}}(\rho)$ from data using transport models.

Probing the Symmetry Energy with the Spectral Pion Ratio

J. Estee,^{1,2,*} W. G. Lynch^{1,2,†} C. Y. Tsang,^{1,2} J. Barney,^{1,2} G. Jhang,¹ M. B. Tsang,^{1,2,‡} R. Wang,¹ M. Kaneko,^{3,4} J. W. Lee,⁵
 T. Isobe,^{3,§} M. Kurata-Nishimura,³ T. Murakami,^{3,4,||} D. S. Ahn,³ L. Atar,^{6,7} T. Aumann,^{6,7} H. Baba,³ K. Boretzky,⁷
 J. Brzychczyk,⁸ G. Cerizza,¹ N. Chiga,³ N. Fukuda,³ I. Gasparic,^{9,3,6} B. Hong,⁵ A. Horvat,^{6,7} K. Ieki,¹⁰ N. Inabe,³
 Y. J. Kim,¹¹ T. Kobayashi,¹² Y. Kondo,¹³ P. Lasko,¹⁴ H. S. Lee,¹¹ Y. Leifels,⁷ J. Łukasik,¹⁴ J. Manfredi,^{1,2} A. B. McIntosh,¹⁵
 P. Morfouace,¹ T. Nakamura,¹³ N. Nakatsuka,^{3,4} S. Nishimura,³ H. Otsu,³ P. Pawłowski,¹⁴ K. Pelczar,⁸ D. Rossi,⁶
 H. Sakurai,³ C. Santamaria,¹ H. Sato,³ H. Scheit,⁶ R. Shane,¹ Y. Shimizu,³ H. Simon,⁷ A. Snoch,¹⁶ A. Sochocka,⁸
 T. Sumikama,³ H. Suzuki,³ D. Suzuki,³ H. Takeda,³ S. Tangwanchaoen,¹ H. Toernqvist,^{6,7} Y. Togano,¹⁰ Z. G. Xiao,¹⁷
 S. J. Yennello,^{15,18} and Y. Zhang¹⁷

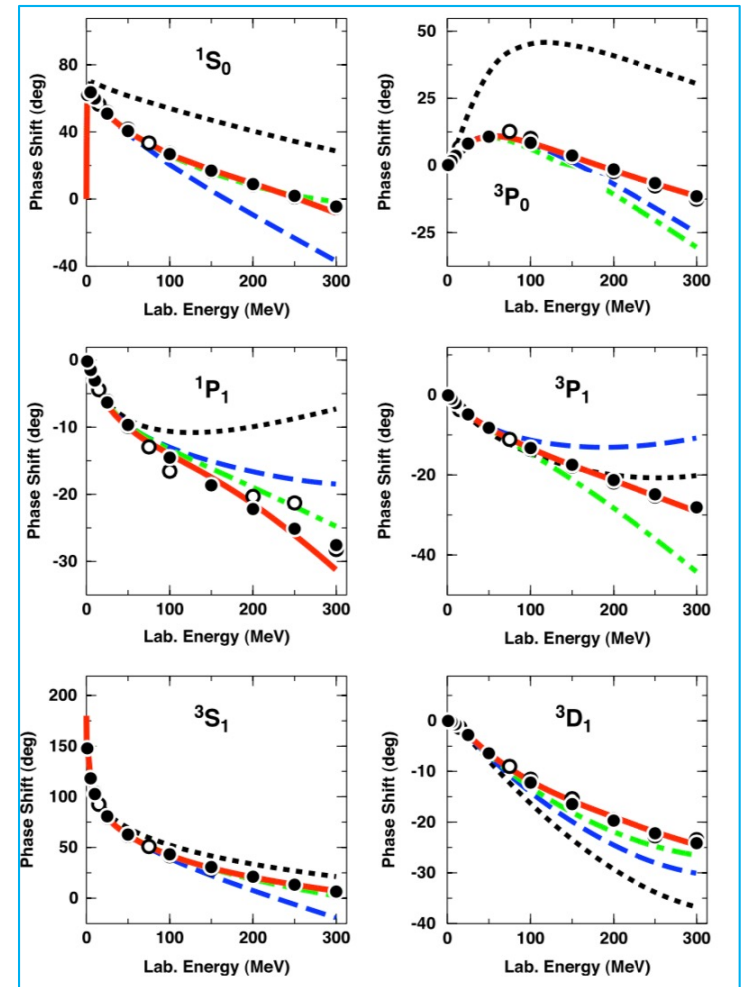
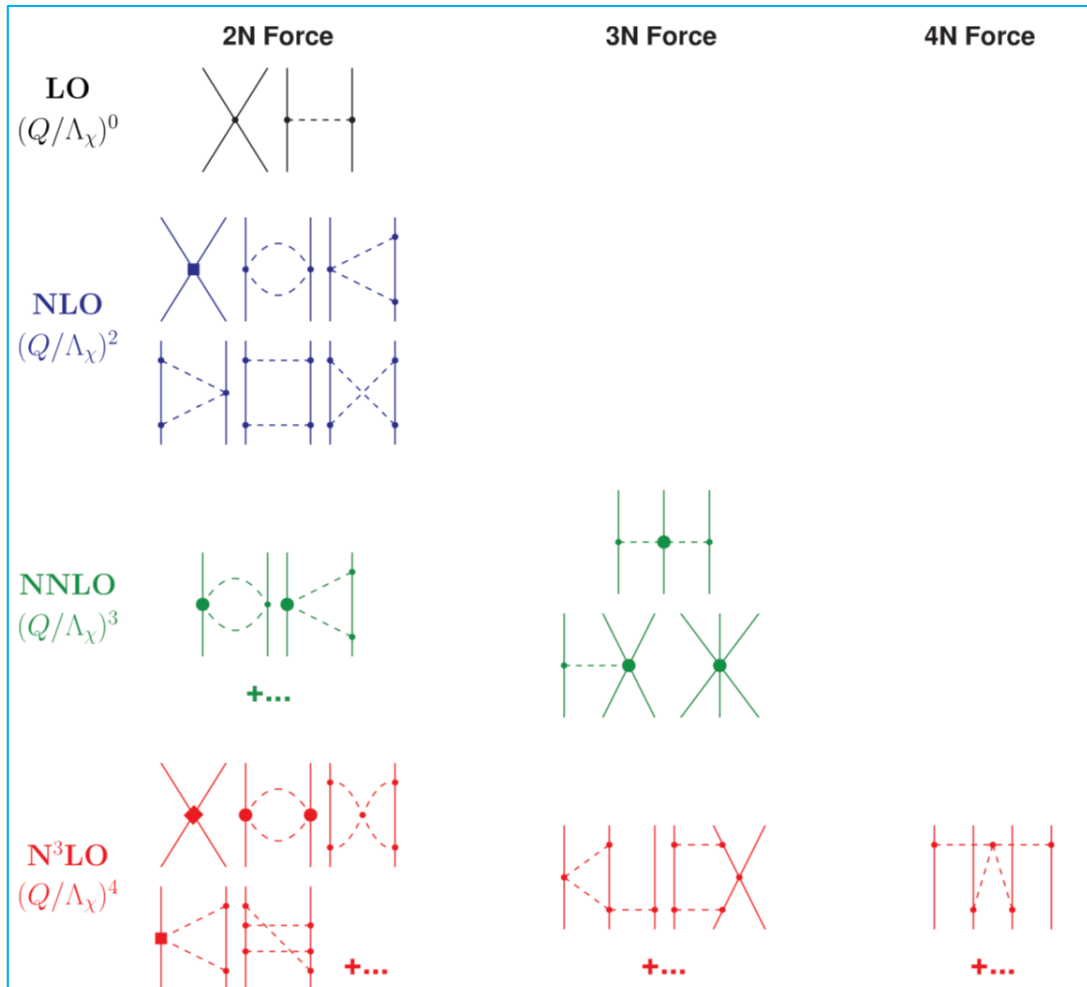
(S π RIT Collaboration)



Correlation contours between L and $\Delta m_{np}^*/\delta$ extracted from the single spectral ratio of the neutron rich $^{132}\text{Sn}+^{124}\text{Sn}$ and near symmetric $^{108}\text{Sn}+^{112}\text{Sn}$ reactions. The green shaded region lies within 68% confidence level for data with $p_T > 200$ MeV/c. The dotted blue lines denote contours corresponding to the 95% confidence level. $\rightarrow S_0 = 38.3 \pm 4.7$ MeV, $L = 106 \pm 37$ MeV.

Chiral nucleon-nucleon forces

Machleidt & Entem, Physics reports 503, 1 (2011)



■ Fit measured phase shifts well

Selfconsistent Green's function method

W. H. Dickhoff and C. Barbieri, Prog. Part. Nucl. Phys. **52**, 377 (2004).

A. Rios, A. Polls, and I. Vidaña, Phys. Rev. C **79**, 025802 (2009).

Dyson's equation $G(\mathbf{p}, \omega) = G_0(\mathbf{p}, \omega) + G_0(\mathbf{p}, \omega)\Sigma^*(\mathbf{p}, \omega)G(\mathbf{p}, \omega)$

Nucleon spectral function $A(\mathbf{p}, \omega) \sim \text{Im}\Sigma^*(\mathbf{p}, \omega)$

Nucleon occupation number $n(\mathbf{p}) = \int \frac{d\omega}{2\pi} \mathcal{A}(\mathbf{p}, \omega) f(\omega)$

Energy per nucleon (Equation of state)

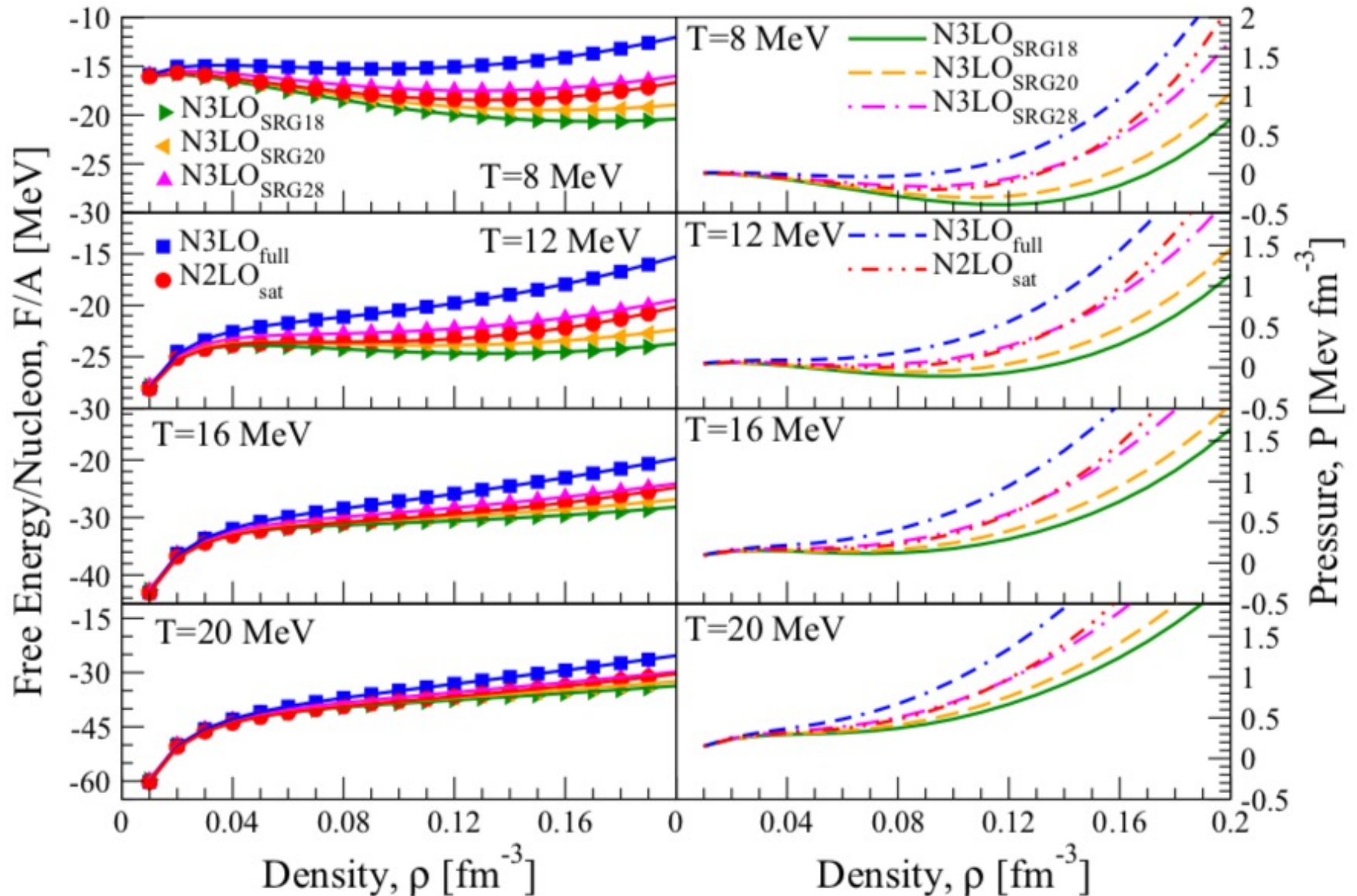
Fermi-Dirac distribution

$$\frac{E}{A} = \frac{\nu}{\rho} \int \frac{d\mathbf{p}}{(2\pi)^3} \int \frac{d\omega}{2\pi} \frac{1}{2} \left(\frac{p^2}{2m} + \omega \right) \mathcal{A}(\mathbf{p}, \omega) f(\omega) - \frac{1}{2} \langle \hat{W} \rangle$$

Three-body contribution

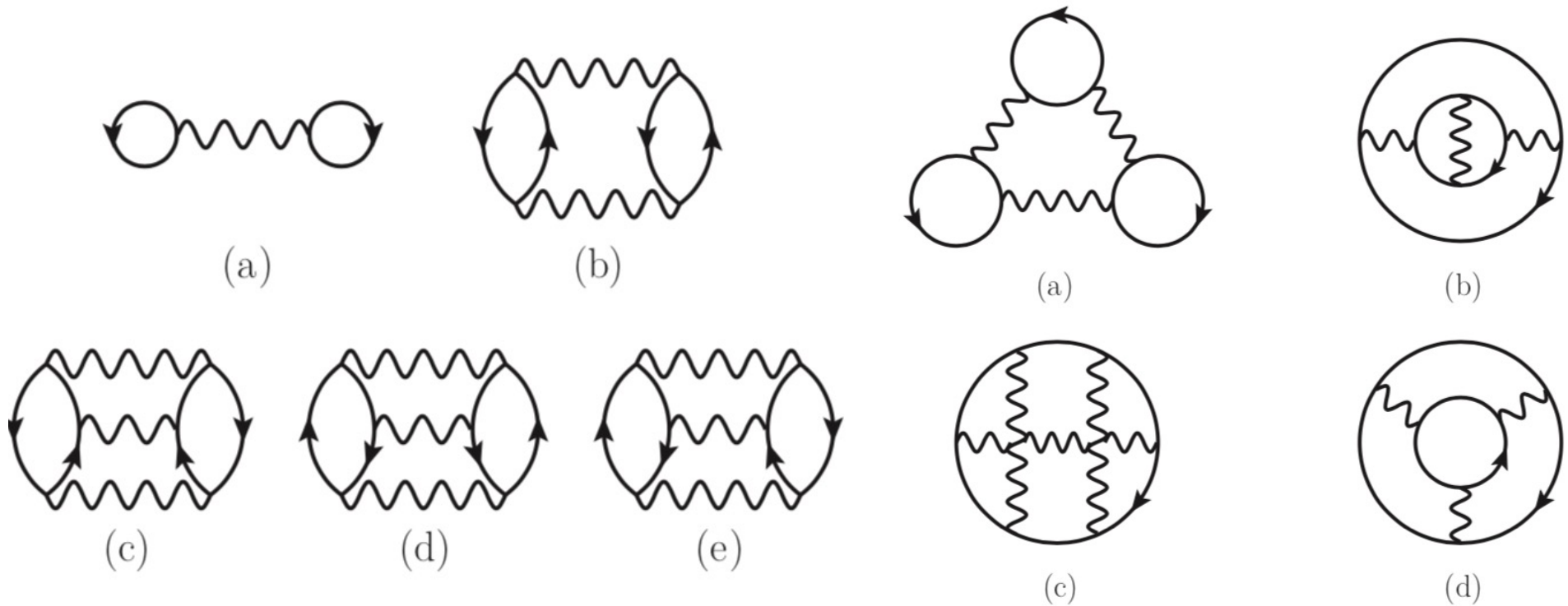
Nuclear equation of state at different temperatures

Carbone, Polls & Rios, PRC 98, 025804 (2018), SCGF approach



Chiral effective many-body perturbation theory

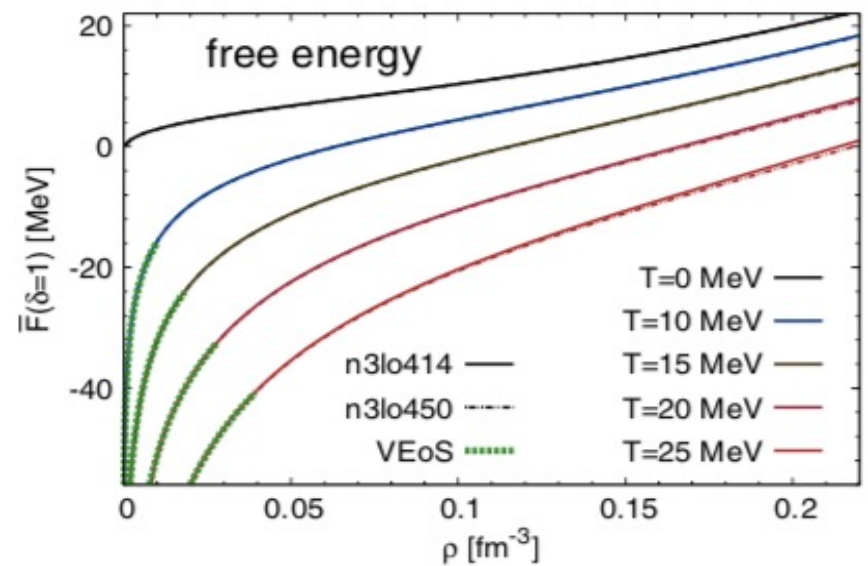
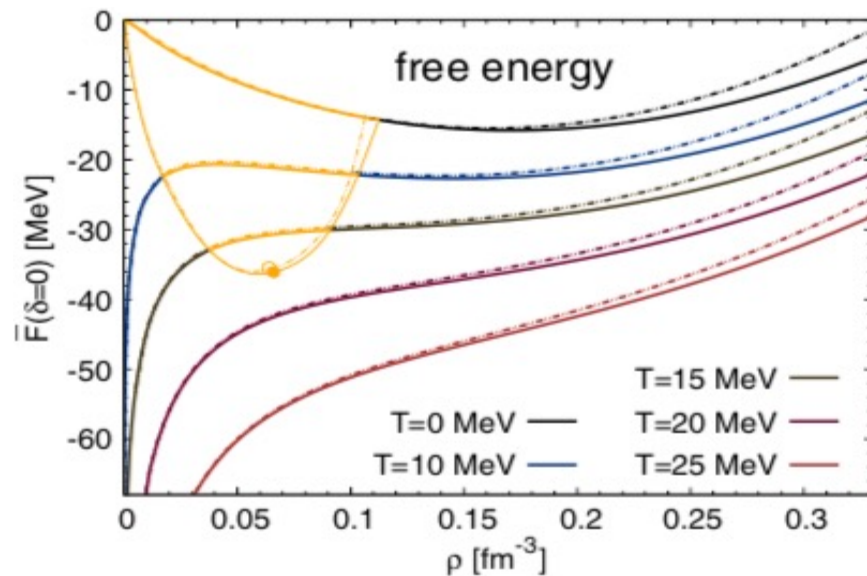
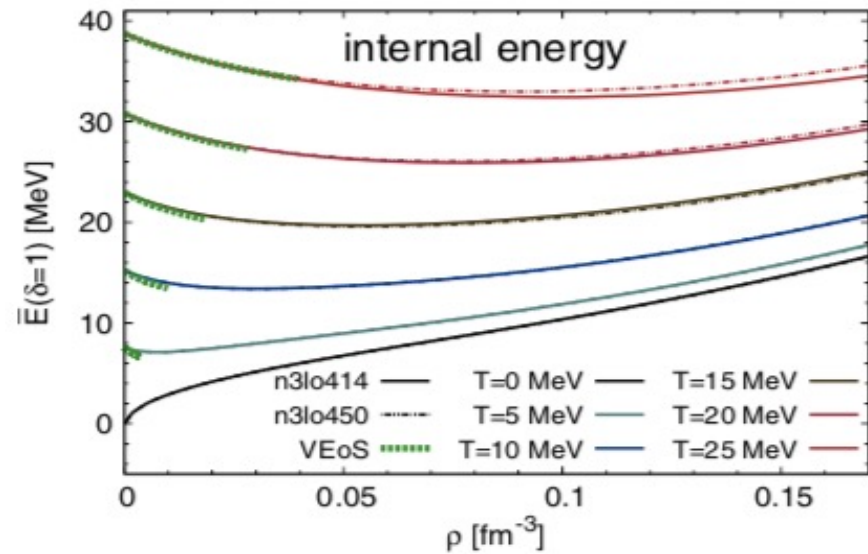
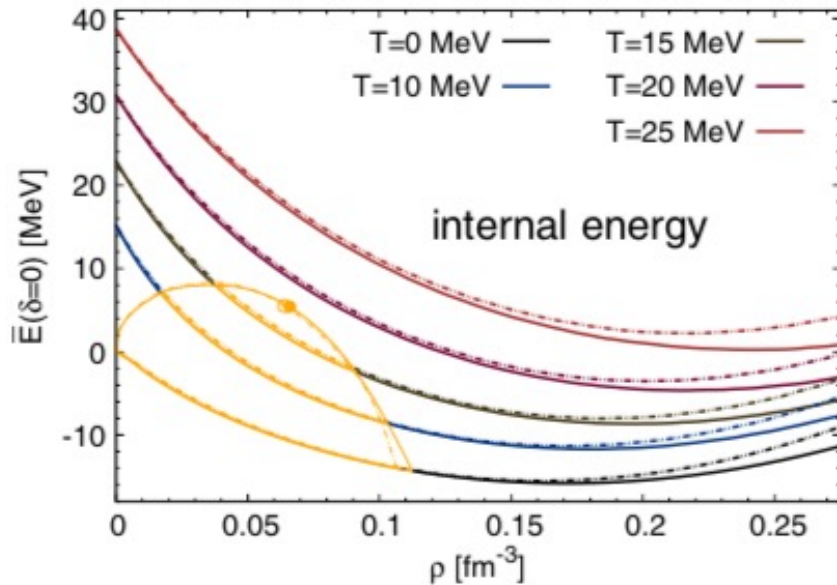
J. W. Holt and N. Kaiser, PRC 95, 034326 (2017)



- The wavy line includes the (antisymmetrized) density-dependent NN interaction derived from the chiral three-body force at N2LO.

Nuclear equation of state at different temperatures

Wellenhofer, Holt & Kaiser, PRC 92, 015801 (2015), Perturbative approach with chiral NN interactions



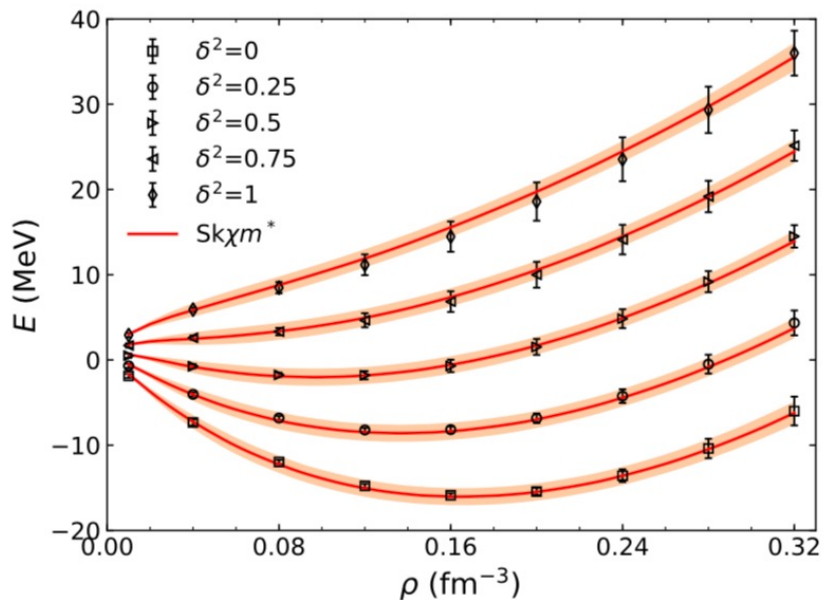
Chiral effective theory inspired transport model χ BUU

- Sk χ m* interaction ($K_0=230$ MeV, $E_{\text{sym}}=31$ MeV, $L=45.6$ MeV)

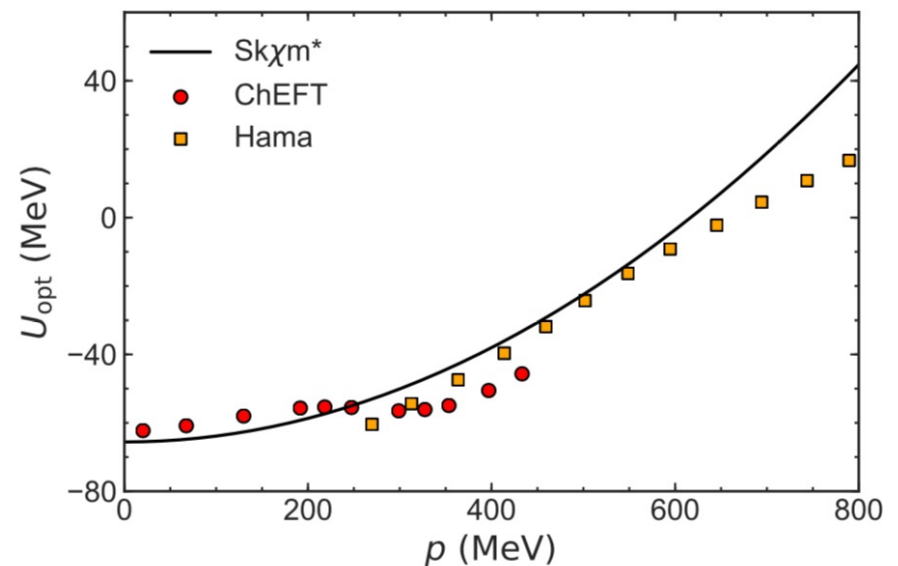
Zhang, Liam, Holt & Ko, PLB 777, 73 (2018)

$$\begin{aligned}
 v(\mathbf{r}_1, \mathbf{r}_2) = & t_0(1 + x_0 P_\sigma)\delta(\mathbf{r}_1 - \mathbf{r}_2) + \frac{1}{2}\mathbf{t}_1(\mathbf{1} + \mathbf{x}_1\mathbf{P}_\sigma)[\mathbf{k}'^2\delta(\mathbf{r}_1 - \mathbf{r}_2) + \text{c.c.}] \\
 & + t_2(1 + x_2 P_\sigma)\mathbf{k}' \cdot \delta(\mathbf{r}_1 - \mathbf{r}_2)\mathbf{k} + \frac{1}{6}\mathbf{t}_3(\mathbf{1} + \mathbf{x}_3\mathbf{P}_\sigma)\rho^\alpha \left(\frac{\mathbf{r}_1 + \mathbf{r}_2}{2}\right) \delta(\mathbf{r}_1 - \mathbf{r}_2) \\
 & + iW_0(\sigma_1 + \sigma_2) \cdot [\mathbf{k}' \times \delta(\mathbf{r}_1 - \mathbf{r}_2)\mathbf{k}]
 \end{aligned}$$

- Parameters fitted to EOS from chiral effective theory and binding energies of 7 doubly magic nuclei



- Good description of momentum dependence of optical potential below 600 MeV, dipole polarizability, and neutron skin thickness



Improved momentum-dependent density functional

J. Xu, L. W. Chen, and B. A. Li, Phys. Rev. C **91**, 014611 (2015)

$$V_{\text{ImMDI}} = \frac{A_u \rho_n \rho_p}{\rho_0} + \frac{A_l}{2\rho_0} (\rho_n^2 + \rho_p^2) + \frac{B}{\sigma + 1} \frac{\rho^{\sigma+1}}{\rho_0^\sigma} (1 - x\delta^2) \\ + \frac{1}{\rho_0} \sum_{q,q'} C_{q,q'} \int \int d^3p d^3p' \frac{f_q(\vec{r}, \vec{p}) f_{q'}(\vec{r}, \vec{p}')}{1 + (\vec{p} - \vec{p}')^2 / \Lambda^2}$$

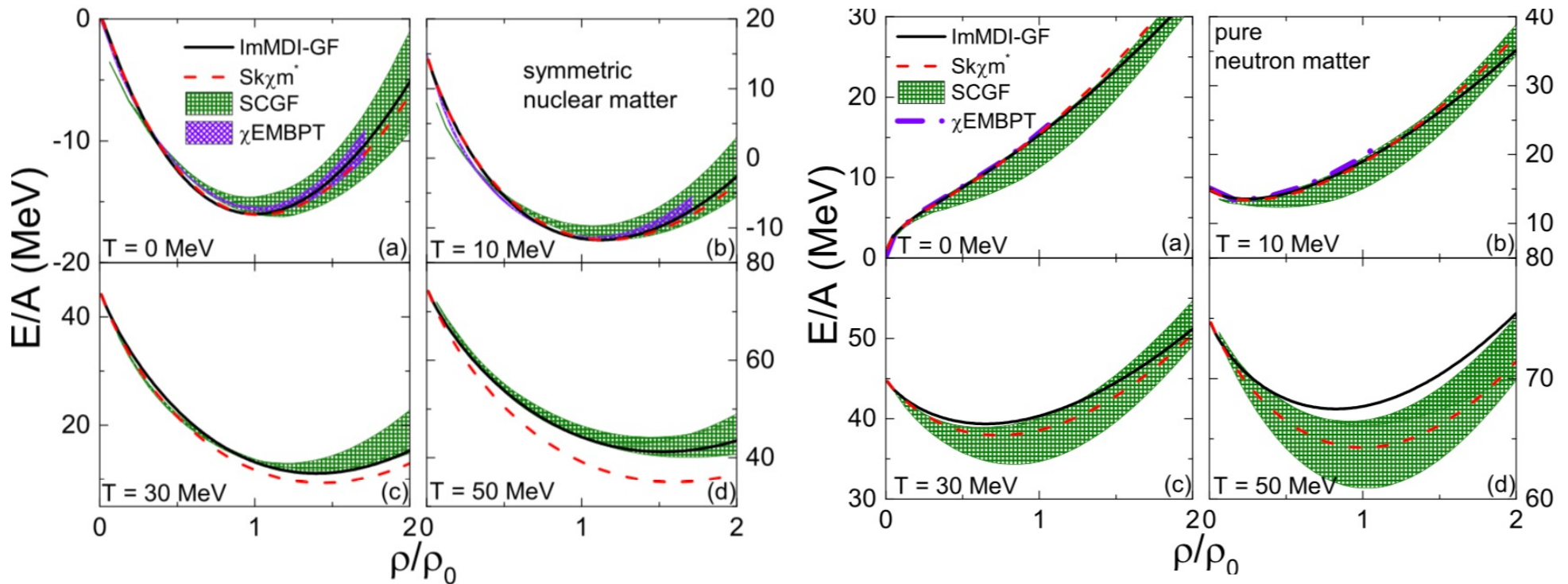
$$A_l(x, y) = A_0 + y + x \frac{2B}{\sigma + 1}, \quad A_u(x, y) = A_0 - y - x \frac{2B}{\sigma + 1}$$

$$C_{q,q}(y) = C_{l0} - 2(y - 2z) \frac{p_{f0}^2}{\Lambda^2 \ln[(4p_{f0}^2 + \Lambda^2)/\Lambda^2]}$$

$$C_{q,-q}(y) = C_{u0} + 2(y - 2z) \frac{p_{f0}^2}{\Lambda^2 \ln[(4p_{f0}^2 + \Lambda^2)/\Lambda^2]}$$

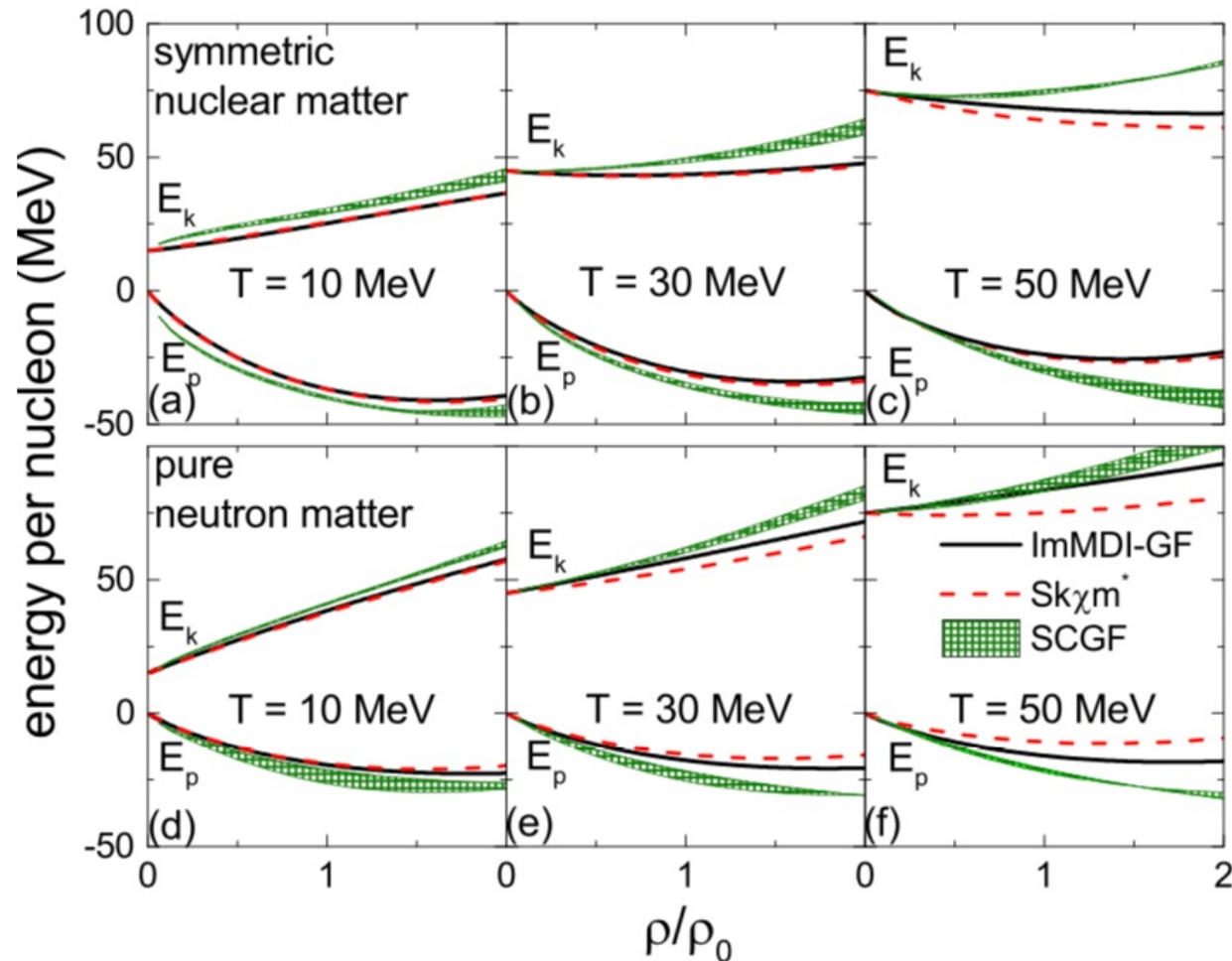
- Fit to empirical energy dependence of single nucleon potential from Hama et al. [PRC 41, 2737 (1990), 47, 297 (1993)].

Nuclear matter equation of state at different temperatures



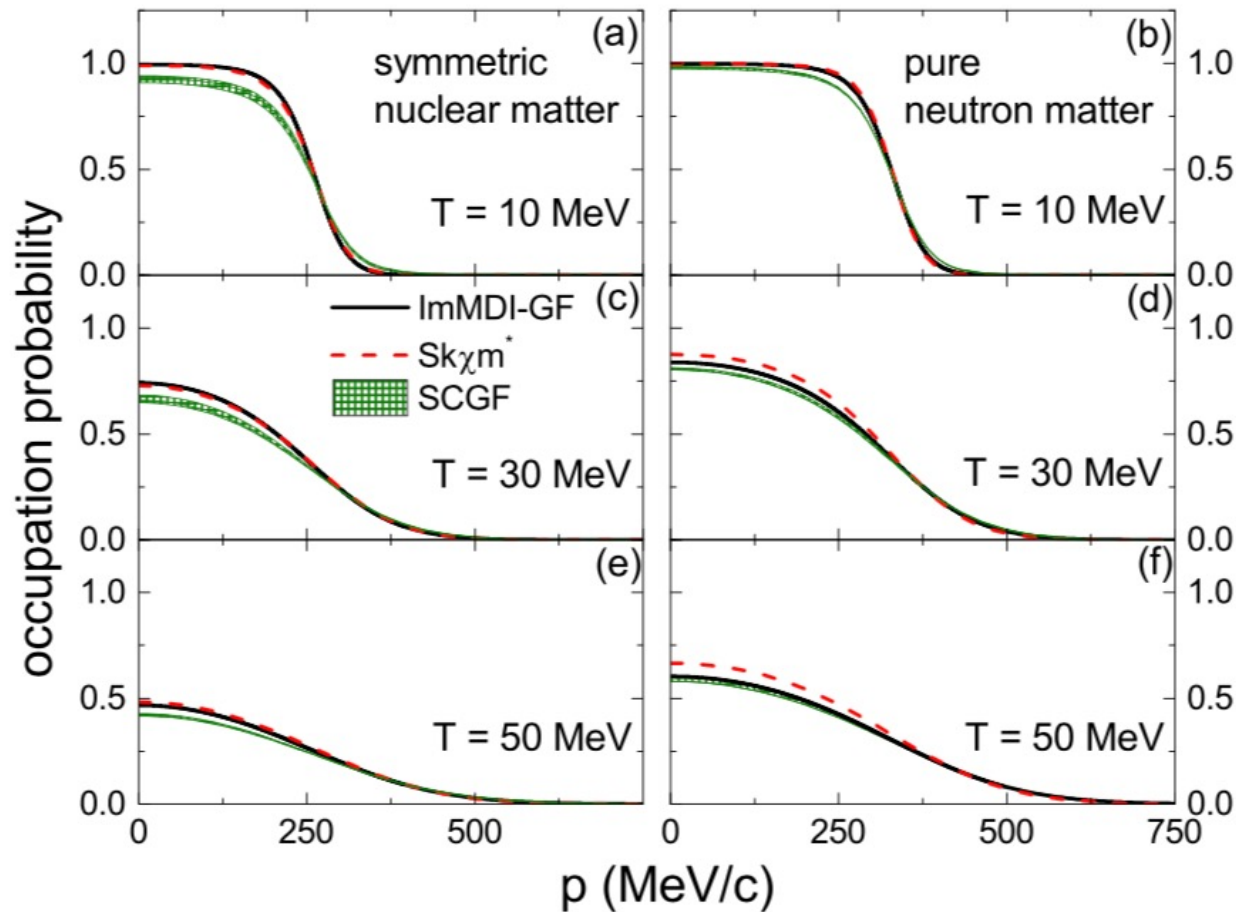
- In SNM, ImMDI-GF agrees with both SCGF and χ EMBPT, which are consistent within their uncertainties, at all temperatures but Sk χ m* starts to deviate as temperature of SNM increases.
- In PNM, Sk χ m* does better at high temperature.

Kinetic energy and potential energy per nucleon



- SCGF has a larger kinetic energy due to smaller occupation number at low momentum as a result of correlations.
- ImMDI-GF and $Sk\chi m^*$ have similar potential energy in SNM but differ in PNM due to different occupation numbers, and both higher than SCGF.

Nucleon number occupation number at normal density

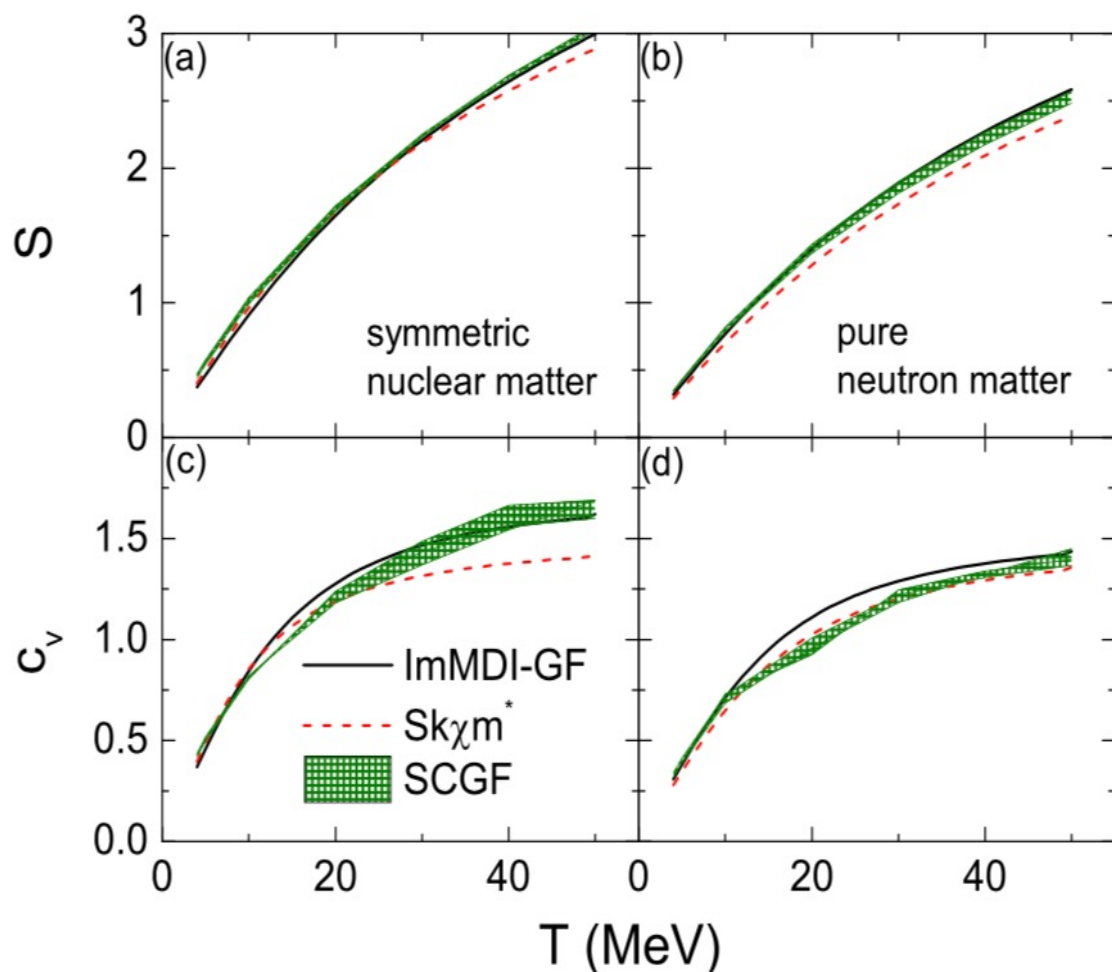


- Depletion of low momentum nucleons in SNM from SCGF due to correlation effects.
- More low momentum nucleons from Sk χ m* in PNM at high temperature due to strong quadratic momentum dependence.

Entropy per nucleon and heat capacity

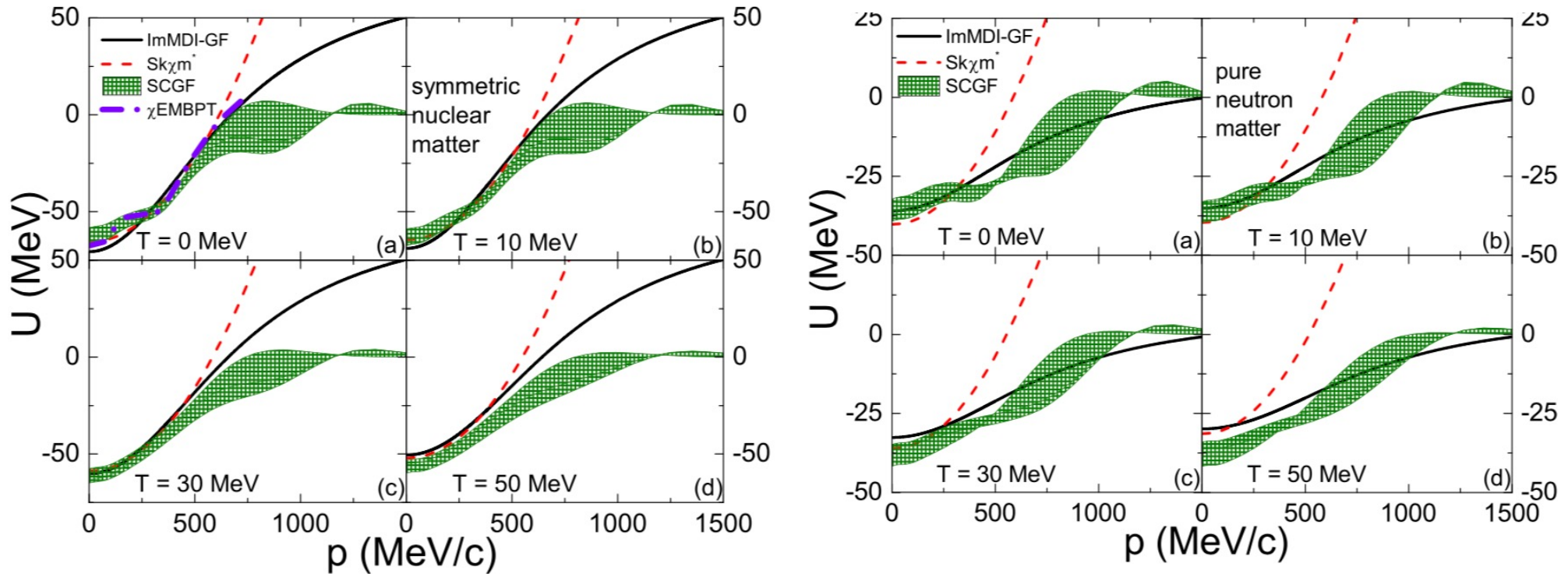
$$\text{Entropy } S = -\frac{\nu}{\rho} \int \frac{d^3p}{(2\pi)^3} [n \ln n + (1 - n) \ln(1 - n)]$$

$$\text{Heat capacity } c_v = T \left(\frac{\partial S}{\partial T} \right)_{\delta, \rho}$$



- Larger entropy from SCGF due to correlations.
- Smaller entropy from Sk χ m* due to sharper nucleon momentum distribution, and thus smaller heat capacity at larger momentum.

Momentum dependence of mean-field potential in nuclear matter at different temperatures



- In SNM, both ImMDI-GF and $Sk\chi m^*$ have too strong momentum dependence than both SCGF and $\chi EMBPT$, with $Sk\chi m^*$ even stronger due to its quadratic dependence.
- In PNM, ImMDI-GF agrees with both SCGF and $\chi EMBPT$ but $Sk\chi m^*$ remains too strong.

Pion production from $^{197}\text{Au}+^{197}\text{Au}$ collisions in χBUU

TABLE II: π^- and π^+ yields in $^{197}\text{Au}+^{197}\text{Au}$ collisions at the impact parameter of 1 fm and the incident energy of $E/A=400$ MeV. Experimental data from the FOPI Collaboration [50] are also listed for comparison. (Without pion potentials)

	FOPI [50]	free	Sk χm^*	
		$A = 0$	$A = 0$	$A = 1.9$
π^-	2.80(14)	2.70(3)	7.84(4)	2.96(2)
π^+	0.95(8)	0.90(2)	2.57(2)	0.92(1)
$\pi^- + \pi^+$	3.75(22)	3.60(5)	10.41(6)	3.88(3)
π^- / π^+	2.95(29)	3.02(6)	3.05(3)	3.2(5)

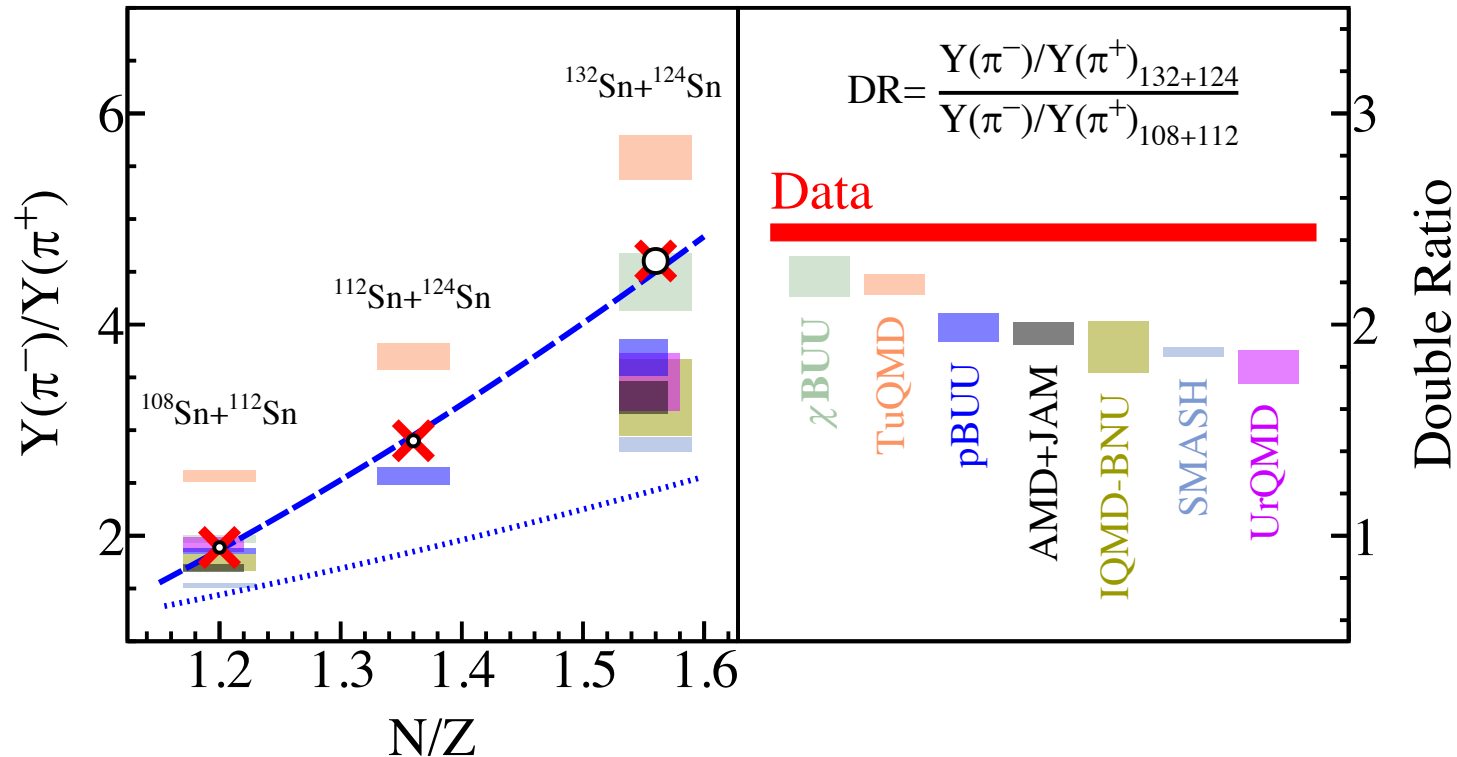
$$\sigma_{NN \rightarrow N\Delta}(\rho) = \sigma_{NN \rightarrow N\Delta}(0) \exp(-A\rho_N/\rho_0).$$

- Without mean-field effects in collision terms can describe data.
- With mean-field effects in collision terms overestimates total pion yield, although give reasonable charged pion ratio.
- Introducing also reduced cross section for $NN \rightarrow N\Delta$ in medium can also reproduce data.

Pion production in $^{132}\text{Sn} + ^{124}\text{Sn}$ and $^{112}\text{Sn} + ^{108}\text{Sn}$ at 270A MeV

G. Jhang et al. (S π RIT, TMEP), Phys. Lett. B 813, 136016 (2021)

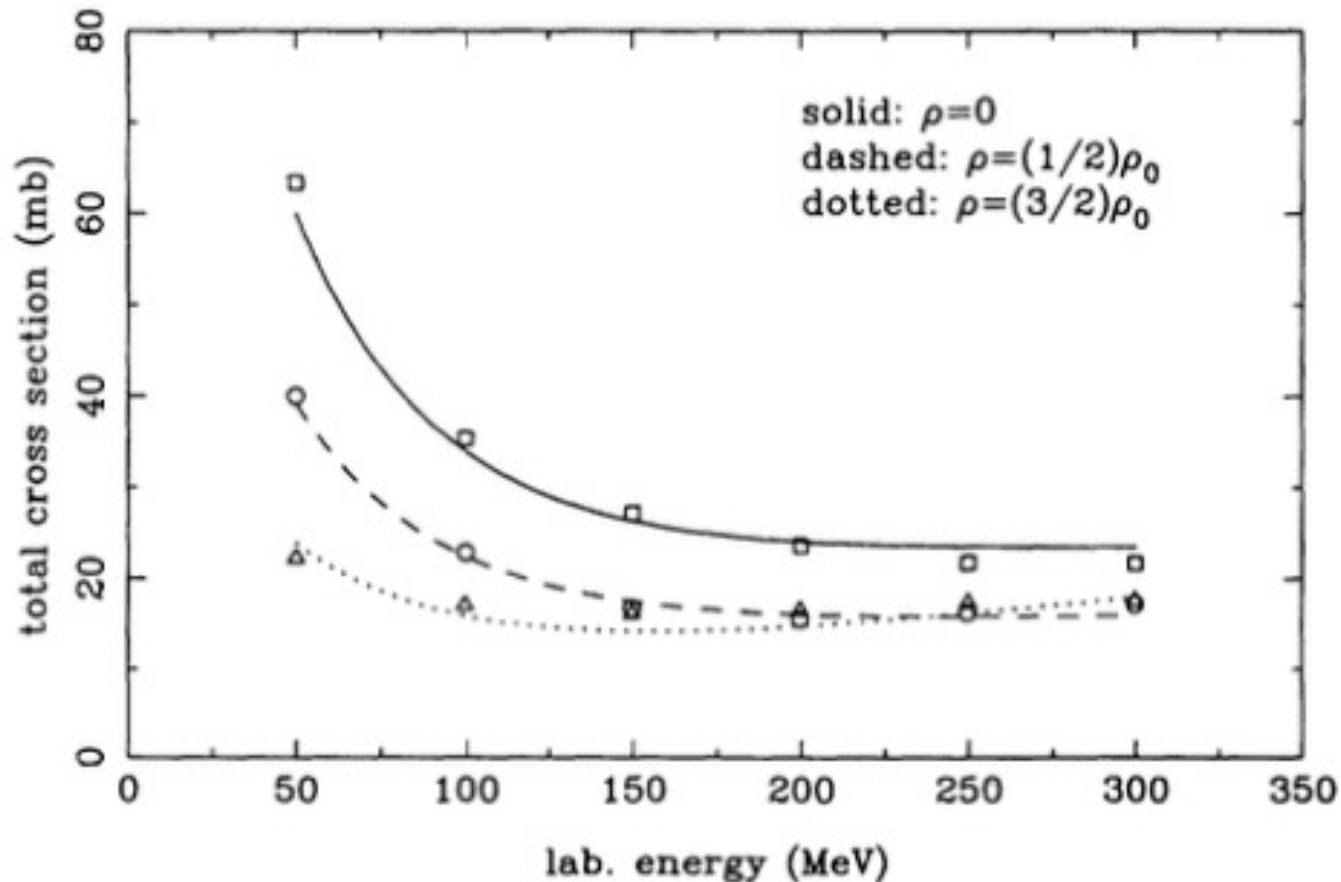
- Momentum-independent mean fields; stiff and soft symmetry energy; self-consistent initial distributions; constant BB elastic scattering cross section ($\sigma = 40$ mb); $NN \leftrightarrow N\Delta$ and $\Delta \leftrightarrow N\pi$.
- Assess uncertainties on pion yield among codes and establish likelihood for extracting stiffness of nuclear symmetry energy from charged pion ratio.



Although no transport models can perfectly describe the data yet, the symmetry energy effect in some models is larger than the experimental errors.

In-medium nucleon-nucleon scattering cross sections

Machleidt & Li, PRC 49, 566 (1994)



- Based on Bonn meson-exchange nucleon-nucleon potential.
- Strong decrease of NN cross section with increasing density.
- Need temperature and isospin asymmetry dependence, which can be similarly obtained from the chiral nucleon-nucleon interactions.

Summary

- Heavy ion collisions have made it possible to study the properties of strong-interaction matter
 - Low energies \rightarrow strong dissipation of ~ 15 MeV/fm in nuclear collective motion
 - High energies \rightarrow isoscalar incompressibility $K \sim 210$ -300 MeV
 - With neutron-rich nuclei $\rightarrow E_{\text{sym}}(\rho) \sim 32 (\rho/\rho_0)^\gamma$ with $0.7 < \gamma < 1.1$
for $\rho < 1.2\rho_0 \rightarrow K_{\text{asy}}(\rho_0) \sim -550 \pm 50$ MeV and $L \sim 88 \pm 25$
 - Relativistic energies \rightarrow a strongly coupled quark-gluon plasma
 - Radioactive beam facilities \rightarrow Nuclear symmetry energy at high densities
- Transport models with inputs from chiral effective theory
- Possible test of chiral nuclear interactions at high densities.